α-Aminophosphonates as Potential PARP1 Inhibitors

Schweiker, Stephanie S; Tauber, Amanda L; Kam, Caleb; Eyckens, Daniel J.; Henderson, Luke; Levonis, Stephan M

Published in:
Chemistry Select

DOI:
10.1002/slct.202000520

Published: 08/04/2020

Document Version:
Peer reviewed version

Licence:
Other

DOI: 10.1002/slct.202000520

Communication

Medicinal Chemistry & Drug Discovery

Received: 5.^February.^2020

Accepted: 1.^April.^2020

α-Aminophosphonates as Potential PARP1 Inhibitors

Dr. Stephanie^^S. Schweiker0000-0002-0978-2569,*[a] Amanda^^L. Tauber,[a] Caleb^^M. Kam,[a] Daniel^^J. Eyckens, [b] Dr. Luke^^C. Henderson [b] and Dr. Stephan^^M. Levonis [a]

[a] <orgDiv/>Faculty of Health Sciences and Medicine, <orgName/>Bond University, <city/>Gold Coast, <postCode/>4229, <countryPart/>Queensland, <country/>Australia
E-mail: sschweik@bond.edu.au

[b] <orgName/>Deakin University, <street/>Pigdons Road, <city/>Waurn Ponds Campus, <countryPart/>Geelong, <postCode/>3216, <countryPart/>Victoria <country/>Australia0

<pict> Supporting information for this article is available on the WWW under <url>http://dx.doi.org/10.1002/slct.202000520</url>

α-Aminophosphonates

Binding affinity

DNA damage

Drug discovery

PARP1 inhibitors

PARP1 is well known for binding to damaged DNA and signaling the DNA repair mechanisms within a cell. We propose a new class of PARP1 inhibitors the α–aminophosphonates that target the activation mechanism unique to the PARP1 enzyme. Twenty three Compounds were screened *in silico* for their binding interactions and tested for inhibitory activity against PARP1. Two lead α–Aminophosphonates were identified as effective PARP1 inhibitors.

ADP-ribosyl transferase member 1 (PARP1) is primarily known for its involvement in signaling DNA damage repair mechanisms within a cell. PARP1 inhibitors are used currently for the management of breast cancer (BRCA) gene mutated breast and ovarian cancers. These current generation PARP1 inhibitors are non-selective for PARP1, over the PARP superfamily enzymes. Here we report on a novel class of PARP1 inhibitors, the α-aminophosphonates. α–Aminophosphonates **1--23** were screened *in silico* for their binding interactions and tested for inhibitory activity against PARP1. α–Aminophosphonates **17** and **20** were identified as the most effective PARP1 inhibitors. They inhibited PARP1's activity, at 10^^μM, by 63±3% and 56±3%, respectively.

■ ■ Dear author, Table 3 is missing, please check and correct ■ ■

Introduction

ADP-ribosyl transferase member 1 (PARP1, alternatively named ARTD1) belongs to a family of 18 enzymes which are responsible for catalysing the post-translational addition of ADP-ribose (ADPr) moieties onto target proteins.[1] PARP1 is classified as a poly(ADPr) polymerase (PAR) since it can transfer multiple ADPr units onto a target protein, given NAD is available as a donor. PARP1 is involved in multiple cellular processes, including, binding to and singling the repair of damaged DNA sequences, transcriptional regulation, and cell death signalling.[2] PARP1 is activated when a cell's DNA is damaged. Once activated, PARP1 binds to the damaged DNA and signals the repair mechanism which allows the damaged cells to evade cell death. Other nuclear PARPs, such as PARP2 and PARP3, are also activated upon DNA damage and are also involved in repairing damaged DNA.[3,4]

PARP1 inhibitors have possible applications to treat cancer and inflammatory diseases. They have been shown to be highly successful in the management of BRCA-associated breast and ovarian cancers, as well as in tumours where BRCA genes may be dysfunctional.[5] This is due to an effect know as *synthetic lethality*. Cells possessing the mutated BRCA gene lack the ability to repair DNA breaks by homologous recombination and thus rely on PARP1 to mediate DNA repair. If PARP1 is inhibited, these mutated cells can no longer repair DNA and are cytotoxically affected by the PARP1 inhibition. However, cells not possessing the BRCA mutation are still able to complete DNA repair via the operational BRCA gene.[6]

PARP1 inhibitors have also been shown to be protective in a range of diseases including diabetes, stroke, rheumatoid arthritis, cardiovascular diseases, and inflammatory diseases.[7--9] Currently, there are four FDA approved PARP1 inhibitors on the market, Olaparib, Rucaparib, Niraparib and Talazoparib. There is also another in the late stages of clinical development, Veliparib. All five of these PARP1 inhibitors are nonselective for PARP1 and also inhibit PARP2 with similar potency.[4] However, there is still a drive for the drug discovery of PARP inhibitors. Amongst reported resistance to some of the marketed PARP1 inhibitors [10], a majority of these inhibitors operate in some form, as a nicotinamide mimetic, mirroring the pharmacophoric features as NAD, a ubiquitous coenzyme which is required for many metabolic reactions. As a consequence, many of these NAD analogues that reach clinical trials for PARP1, fail to progress past the early stages due to the

unintentional competition with other cellular pathways that utilise NAD^+ as a cofactor.[11] These interactions with other pathways are often correlated to some of the unwanted side effects and toxicities of PARP1 inhibitors.[4] The concept of a non-NAD-like PARP1 inhibitor that targets the activation mechanism which is unique to the PARP1 enzyme only has the potential to alleviate or reduce these unwanted side effects.[12,13] This paper will report on a novel class of PARP1 inhibitors, the α-aminophosphonates.

α-Aminophosphonate Scaffold

This series of α–Aminophosphonates were computationally analysed in the catalytic domain typically where NAD binds. They possess a phosphonate moiety, similar to NAD, and also have multiple aromatic rings to enhance the pi-pi interactions within the catalytic domain. The compounds had varying nitro, halogen, esters, alkyl and hydroxy groups to further our understanding of the structure activity relationship within the domain.

Docking Results

Compounds **1--23**, synthesised as previously reported[14], were docked into the catalytic domain of PARP1 (4ZZZ.pdb) using PyRx and AutoDock Vina with a root mean square deviation (RMSD)<schr1> between the x-ray crystallographic ligand with the docked pose to be 1.48^^Å. The binding affinity (Kcal/mol) was determined, with a more negative binding affinity being representative of a better fit into the binding pocket. The docked poses were analysed for key molecular interactions (Tables^^1<tabr1><tabr2><tabr3>--4<tabr4>).[15,16] The α-aminophosphonate compounds investigated can be split into three main groups. Those substituted on the original arylamine **1** to **11** (Table^^1<xtabr1>), those substituted on the original aldehyde **12** to **18** (Table^^2<xtabr2>), and the *bis*-α–aminophosphonates **20** to **23** (Table^^3<xtabr3>).<figr1>

Most α-aminophosphonates docked with interaction to Tyr907 and some were situated between the aromatic rings of Tyr907 and Tyr896. α–Aminophosphonate **1** is an example of a compound that is anchored by Tyr907 via a hydrophobic/pi-pi interaction (Figure^^2<figr2>). α–Aminophosphonate **2** displayed a binding affinity of <M->10.4 to PARP1. Upon investigation of the docked poses that a hydrogen bonding was observed to His862 and hydrophobic/pi-pi interaction with Tyr907 (Figure^^2<xfigr2>).

α-Aminophosphonates **5** and **6** when docked with PARP1 both displayed the expected position between Tyr907 and Tyr896 with additional hydrogen bonding observed with **5** to both Asp766 and Arg878 (Figure^^3<figr3>).

Literature has proposed that residue Asp766 may be responsible for the selectivity of PARP1 over PARP2 which was observed in the docked pose of **5** with PARP1.[4] α–Aminophosphonate **14** displayed a binding affinity of <M->9.9 Kcal/mol with positioning between Tyr907 and Tyr896 (Figure^^4<figr4>). Compound **17** displayed a binding affinity to PARP1 with <M->10.3 Kcal/mol. Upon investigation of the docked poses, a hydrogen bonding interaction with Glu763 was observed. However, hydrophobic interaction was not evident (Figure^^4<xfigr4>).

Compound **20**, a *bis*-α–aminophosphonate, is much larger than compounds **1** to **18**. Compound **20**, when docked into the PARP1 catalytic domain, displayed the typical pose consistent with other examples. Compound **20** also displayed the highest binding affinity out of the library with <M->11.2 Kcal/mol to PARP1. Its docked pose revealed a hydrophobic/pi-pi interactions with Tyr896 (Figure^^5<figr5>).

Biological Evaluation in PARP1 Assay

Seven of the docked α-aminophosphonates (**1**, **2**, **5**, **6**, **14**, **17**, and **20**) were assessed for inhibitory activity against recombinant PARP1 enzyme through a library screening luminescence assay. While these compounds may not represent the most potent of the proposed structures they do represent an excellent cross-section of the structures and substitution patterns possible in this scaffold. The assay was performed at a final PARP1 concentration of 2.5 ng/μL and compound concentration of 10^^μM.

The assay included a blank representing full inhibition of the PARP1 enzymes and a positive control representing no PARP1. Compound **17**, a dichloro-substituted benzaldehyde α-aminophosphonate, was identified as the most effective of the seven assessed compounds, inhibiting PARP1 by 63±3% (Table^^4<tabr4>). The docked pose of **17** showed hydrogen bonding interactions with Glu763.

The following three compounds, **20**, **2**, and **5** all fell within similar inhibitory range with percentage inhibition values of 56±3%, 52±3%, and 50±2%, respectively for the three (Table^^4<xtabr4>). Structurally, compounds **2** and **5** differ only in the substitution of the 4-nitro

versus a 3-ether group, and compound **20** being the bis α-aminophosphonate form of compound **5**. Compounds **2**, **5**, and **20** displayed very good binding affinities (-10.4, <M->10.6 and <M->11.2, respectively) *in silico* and all showed hydrogen bonding interactions.

The final three compounds assessed, compound **14** with a nitro substituted benzaldehyde α-aminophosphonate, compound **6** with a bromine substituted amine α-aminophosphonate, and **1** an unsubstituted benzaldehyde α-aminophosphonate appeared the least effective of the series, only inhibiting PARP1 by 31±1% for **6** and 32±1% for **1** (Table^^4<xtabr4>). Comparison of the assay results with the docked poses showed that compounds **14**, **6**, and **1** which had lower percent inhibition also displayed good binding affinities (-9.9, <M->10.7 and <M->10.0, respectively) but they did not have any hydrogen bonding interactions only one hydrophobic/pi-pi interaction with Tyr907.

Conclusion

α–Aminophosphonates **1--23** were screened *in silico* for binding affinity and key residue interaction with PARP1. Compounds **1**, **2**, **5**, **6**, **14**, **17**, and **20** were then tested for inhibitory activity against PARP1 through a library screening luminescence assay. Compound **17**, a dichloro-substituted benzaldehyde α-aminophosphonate, was identified as the most effective PARP1 inhibitor by inhibiting PARP1's by 63±3% at 10^^μM. Compound **20**, a bis-α–aminophosphonate, was identified as a moderate PARP1 inhibitor with 56±3% inhibition at 10^^μM.

Experimental

Docking Studies

The crystal structure of PARP1 (4ZZZ.pdb) was obtained from the Protein Data Bank (http://www.rcsb.org/pdb/). Prior to docking, the ligands were extracted from the crystal structure and water molecules were removed. The compounds were drawn in ChemDraw, which then it was exported to UCSF Chimera for structural editing and energy minimization. Edited molecules are then imported into PyRx for docking with the corresponding macromolecules from previous step. The docking pose was then saved as a .pdb then imported into Chimera along with the macromolecule for visualization.

PARP1 Inhibition Assay

Following the protocol outlined by the BPS Biosciences PARP1 chemiluminescent assay

kit, the compounds were prepared in dimethyl sulfoxide and diluted with PARP buffer and water to a stock concentration of 100^^μM (BPS Biosciences). For the PARP1 assay, 25 μL of master mixture (80% water, 10% concentrated PARP buffer, 10% Opti-PARP assay mixture), 20 μL PARP1 (2.5 ng/μL) and 5 μL of the diluted compounds were added to each of the histone-soaked wells for a final inhibitor concentration of 10^^μM. Each sample was repeated in triplicates, along with a positive control containing no test-sample and the blank sample containing no PARP1. The results were collected as luminesce before being adjusted to the blank and reported as a 100% minus the percentage of the mean positive control along with the standard error. This provided a value where 0%=positive control or no inhibition and 100%=blank or full inhibition.

Supporting information

There is no supporting information with this document.

Conflict of Interest

The authors declare no conflict of interest.

<lit1><jnl>S.^^S. Schweiker, A.^^L. Tauber, M.^^E. Sherry, S.^^M. Levonis, *MiniRev. Med. Chem.* **2018**, *18*), 1659--1669</jnl>.

<lit2><jnl>R. Gupte, Z. Liu, W.^^L. Kraus, *Genes Dev.* **2017**, *31*, 101--126</jnl>.

<lit3><jnl>M.^^F. Langelier, D.^^D. Ruhl, J.^^L. Planck, W.^^L. Kraus, J.^^M. Pascal, J. Biol, *Chem.* **2010**, *285*, 18877--18887</jnl>.

<lit4><jnl>P.^^G. Jain, B.^^D. Patel, *Eur. J. Med. Chem.* **2019**, *165*, 198--215</jnl>.

<lit5><jnl>C. Underhill, M. Toulmonde, H. Bonnefoi, *Ann. Oncol.* **2011**, *22*, 268--279</jnl>.

<lit6><jnl>H. Farmer, N. McCabe, C.^^J. Lord, A.^^N. Tutt, D.^^A. Johnson, T.^^B. Richardson, M. Santarosa, K.^^J. Dillon, I. Hickson, C. Knights, N.^^M. Martin, S.^^P. Jackson, G.^^C. Smith, A. Ashworth, *Nature* **2005**, *434*, 917--921</jnl>.

<lit7><jnl>M. Klofers, J. Kohaut, I. Bendix, J. Herz, V. Boos, U. FelderhoffMuser, M. Dzietko, *BioMed Res. Int.* **2017**, *2017*, 11--22</jnl>.

<lit8><jnl>A. Peralta-Leal, J.^^M. Rodríguez-Vargas, R. Aguilar-Quesada, M.^^I. Rodríguez, J.^^L. Linares, M.^^R. de^^Almodóvar, F.^^J. Oliver, *Free Radic. Biol. Med.* **2009**, *47*, 13--26</jnl>.

<lit9><jnl>N.^^A. Berger, V.^^C. Besson, A.^^H. Boulares, A. Bürkle, A. Chiarugi,

R.^^S. Clark, N.^^J. Curtin, S. Cuzzocrea, T.^^M. Dawson, V.^^L. Dawson, G. Haskó, L. Liaudet, F. Moroni, P. Pacher, P. Radermacher, A.^^L. Salzman, S.^^H. Snyder, F.^^G. Soriano, R.^^P. Strosznajder, B. Sümegi, R.^^A. Swanson, C. Szabo, *Br. J. Pharmacol.* **2018**, *175*, 192--222</jnl>.

<lit10><jnl>S.^^L. Edwards, R. Brough, C.^^J. Lord, R. Natrajan, R. Vatcheva, D.^^A. Levine, J. Boyd, J.^^S. Reis-Filho, A. Ashworth, *Nature* **2008**, *451*, 1111</jnl>.

<lit11><jnl>N.^^V. Malyuchenko, E.^^Y. Kotova, O.^^I. Kulaeva, M.^^P. Kirpichnikov, V.^^M. Studitskiy, *Acta Naturae* **2015**, *7*, 27--37</jnl>.

<lit12><jnl>Y. Karpova, C. Wu, A. Divan, M.^^E. McDonnell, E. Hewlett, P. Makhov, J. Gordon, M. Ye, A.^^B. Reitz, W.^^E. Childers, T. Skorski, V. Kolenko, A.^^V. Tulin, *Biochem. Pharmacol.* **2019**, *167*, 149--162</jnl>.

<lit13><jnl>C. Thomas, Y. Ji, N. Lodhi, E. Kotova, A.^^D. Pinnola, K. Golovine, P. Makhov, K. Pechenkina, V. Kolenko, A.^^V. Tulin, *EBioMedicine* **2016**, *13*, 90--98</jnl>.

<lit14><jnl>D.^^J. Eyckens, L.^^C. Henderson, *RSC Advances* **2017**, *7*, 27900--27904</jnl>.

<lit15><jnl>A.^^E. Lohning, S.^^M. Levonis, B. Williams-Noonan, S.^^S. Schweiker, *Curr. med. chem.* **2017**, *17*, 2023--40</jnl>.

<lit16><jnl>S.^^S. Schweiker, S.^^M. Levonis, *Future Med. Chem*. **2020**, *12*, 469--71</jnl>.

<lit17><jnl>T.^^A. Hopkins, W.^^B. Ainsworth, P.^^A. Ellis, C.^^K. Donawho, E.^^L. Digiammarino, S.^^C. Panchal, V.^^C. Abraham, M.^^A. Algire, Y. Shi, A.^^M. Olson, E.^^F. Johnson, J.^^L. Wilsbacher, D. Maag, *Mol. cancer res.* **2019**, *17*, 409--419</jnl>.

<lit18><other>European Medicines Agency, **2017**, *648982*, 1--122</other>.

Scheme^^1 Synthesis of the α-aminophosphonate scaffold, derived from an amine (in red), aldehyde (in blue) and the diphenylphosphite (in black).

Figure^^1 Known PARP1 inhibitor Olaparib® and Nicotinamide adenine dinucleotide (NAD^+) chemical structure.

Figure^^2 Compound **1** (blue, LHS) and compound **2** (purple/grey, RHS) docked into the catalytic domain of PARP1 with binding affinities

(-10.0 Kcal/mol and <M->10.4 Kcal/mol respectively) binding interactions included being positioned between the Tyr902 and His862 with hydrogen bonding to residue His862 observed for compound **2**.

Figure^^3 Compound **5** (Orange, LHS, binding affinity <M->10.6 Kcal/mol) and **6** (blue, RHS, binding affinity <M->10.7 Kcal/mol) in PARP1. Both compounds displaying the key position between residues Tyr907 and Tyr896. Compounds **5** also displayed hydrogen bonding with Arg878 (displayed in red).

Figure^^4 Compound **14** (hot pink, LHS, <M->9.9 Kcal/mol) docking into PARP1 with typical binding interactions with Tyr907. Compound **17** (purple, RHS, binding affinity <M->10.3 Kcal/mol) docked into PARP 1 catalytic domain with hydrophobic binding interactions sandwiching the compound between the Tyr907 and Tyr896 residues and hydrogen bonding to Glu763 (displayed in red).

Figure^^5 Compound 20 (green) docked into the PARP1 catalytic domain. Binding interactions Pi with Tyr896. Both were also positioned between the Tyr907 and Tyr896 residues.

Table^^1 Structure and docking results of substituted amine α–aminophosphonates **1** to **11**. Binding affinity (Kcal/mol), hydrogen bonding (HB) interactions and hydrophobic/pi-pi (Pi) interactions are reported for docking with PARP1.

<forr3>

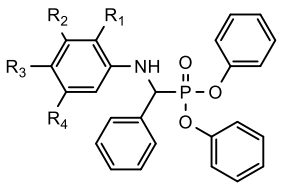

Cpd	R_1	R_2	R_3	R_4	Binding affinity (Kcal/mol)[a]	Binding Interactions and type[b]
1	H	H	H	H	-10.0	Pi Tyr907
2	H	OEt	H	H	-10.4	HB His862 Pi Tyr907
3	H	H	F	H	-10.3	HB Glu763 Pi Tyr907
4	H	H	Cl	H	-10.4	Pi Tyr907
5	H	H	NO_2	H	-10.6	HB Arg878 (x3) HB Asp766 Pi Tyr907
6	Br	H	H	H	-10.7	Pi Tyr907
7	H	H	CO_2H	H	-10.8	HB Ser904 Pi Tyr907
8	H	H	OH	H	-10.2	HB Asp766 Arg878 Pi Tyr907
9	H	Cl	H	H	-10.3	No Evident Interaction
10	H	CF_3	H	H	-11.1	Pi Tyr896 Tyr907
11	H	CF_3	H	CF_3	-11.6	Pi Tyr907

[a] Determined computationally; [b] HB=Hydrogen Bond; Pi=pi-pi interaction

Table^^2 Structure and docking results of substituted benzaldehydes α–aminophosphonates **12** to **17**. Binding affinity (Kcal/mol), hydrogen

bonding (HB) interactions and hydrophobic/pi-pi (Pi) interactions are reported for docking with PARP1.

<forr1>

Cpd	R_1	R_2	R_3	R_4	Binding affinity (Kcal/mol)[a]	Binding Interactions and type[b]
12	H	H	CH_3	H	-10.5	Pi Tyr907, Tyr896
13	H	H	Br	H	-10.2	Pi Tyr907
14	H	H	NO_2	H	-9.9	Pi Tyr907
15	H	H	F	H	-10.8	Pi Tyr907
16	OH	H	H	H	-10.5	Pi Tyr907, Tyr896
17	H	Cl	Cl	H	-10.3	HB Glu763
18	H	H	H	H	-10.6	HB Tyr896 Pi Tyr907
19	H	H			-10.2	HB Asp766 Pi Tyr907
20	NO_2	NO_2			-11.2	Pi Tyr896
21	Br	Br			-10.9	No Evident Interaction
22	CH_3	CH_3			-10.3	No Evident Interaction
23	CH_3	H			-10.4	Pi Tyr907

[a] Determined computationally; [b] HB=Hydrogen Bond; Pi=pi-pi interaction

Table^^3 Structure and docking results of bis-α–aminophosphonates **19** to **23**. Binding affinity (Kcal/mol), hydrogen bonding (HB) interactions and hydrophobic/pi-pi (Pi) interactions are reported for docking with PARP1.

<forr2>

Table^^4 Percentage inhibition data of α-aminophosphonates (**1**, **2**, **5**, **6**, **14**, **17**, and **20**) and previously reported IC_{50} of common PARP1 inhibitors Olaparib, Rucaparib, Veliparib and Talazoparib[17] and Niraprib[18]. Luminescence values are adjusted to the blank sample (full inhibition) and shown as a percentage inhibition. (n=3, ± SEM). All tested compounds were significantly different from both the positive control and blank ($p < 0.0001$).

Compound	PARP1% inhibition or IC_{50}
1	32% ±1%
2	52% ±3%
5	50% ±2%
6	31% ±1%
14	46% ±2%
17	63% ±3%

20	56% ±3%
Olaparib	0.47 ±0.04
Rucaparib	0.38 ±0.01
Niraparib	3.76 ±1.6
Veliparib	1.05 ±0.4
Talazoparib	0.50 ±0.03